UCRL-JRNL-203968

LAWRENCE
LIVERMORE
NATIONAL
LABORATORY

Titan's 2 micron Surface Albedo and Haze Optical Depth in 1996-2004

S.G. Gibbard, I. de Pater, B.A. Macintosh, H.G. Roe, C.E. Max, E.F. Young, C.P. McKay

May 4, 2004

Geophysical Research Letters

Disclaimer

TITAN'S 2 μm SURFACE ALBEDO AND HAZE OPTICAL DEPTH IN 1996-2004

S.G. Gibbard[1], I. de Pater[2], B.A. Macintosh[1], H.G. Roe[3], C.E. Max[1,4], E.F. Young[5] and C.P. McKay[6]

[1]Institute of Geophysics and Planetary Physics
Lawrence Livermore National Laboratory
Livermore, CA 94550 USA; sgibbard@igpp.llnl.gov
[2] Dept. of Astronomy, University of California at Berkeley
[3]Division of Geological and Planetary Sciences
California Institute of Technology
Pasadena, CA 91125
[4] UCSC NSF Center for Adaptive Optics, Santa Cruz CA 95064
[4] Southwest Research Institute, Boulder, CO 80302
[5] NASA Ames Research Center, Moffett Field, CA 94035

PAPER FOR SPECIAL ISSUE: TITAN: PRE-CASSINI VIEW

ABSTRACT

We observed Titan in 1996-2004 with high-resolution 2 μm speckle and adaptive optics imaging at the W.M. Keck Observatory. By observing in a 2 μm broadband filter we obtain images that have contributions from both Titan's surface and atmosphere. We have modeled Titan's atmosphere using a plane-parallel radiative transfer code that has been corrected to agree with 3-D Monte Carlo predictions. We find that Titan's surface albedo ranges from ≤ 0.02 in the darkest equatorial region of the trailing hemisphere to $\simeq 0.1$ in the brightest areas of the leading hemisphere. Over the past quarter of a Saturnian year haze optical depth in Titan's Southern hemisphere has decreased substantially from a value of 0.48 in 1996 down to 0.18 in 2004, while the northern haze has been increasing over the past few years. As a result of these changes, in 2004 the North/South haze asymmetry at K' band has disappeared.

1 Introduction

Photolysis of methane gas in Titan's stratosphere leads to the production of hydrocarbon haze. The opacity of this haze is such that Titan's surface composition has remained unknown despite decades of observation. Since haze scattering decreases at longer wavelengths, Titan's surface can be probed in the near-infrared through methane absorption 'windows', one of which occurs at wavelengths near 2 μm. Titan's surface has been observed with the HST (Meier *et al.* 2000, Smith *et al.* 1996), with the CFHT using adaptive optics (AO) technology (Coustenis *et al.* 2001, Combes *et al.* 1997), and with the W.M. Keck Telescope using speckle imaging (Gibbard *et al.* 2004, 1999) and adaptive optics (Roe *et al.* 2002, Brown *et al.* 2002).

Broadband filters such as the K' filter that we have used for the observations reported in this letter contain wavelengths that probe the surface and lower atmosphere, as well as wavelengths that probe higher in the atmosphere. Because of this, by using a model of Titan's atmospheric haze we are able to simultaneously construct a surface albedo map and determine atmospheric haze parameters. In an earlier paper (Gibbard *et al.* 1999) we reported the detection of dark areas on Titan's leading hemisphere with a reflectance < 0.05 at 1.6 and 2.1 μm, consistent with the presence of liquid or solid hydrocarbons. We present here a surface albedo map with full longitude coverage, constructed from speckle and adaptive optics observations in 1996-2004. We also present the 2μm haze optical depths derived from the model.

2 Observations and Data Reduction

Speckle and adaptive optics imaging are two different techniques to achieve high (near diffraction limited) spatial resolution. Speckle imaging is a high resolution technique that works well on bright objects such as Titan. The idea is to take very short exposures ($\simeq$ 100 milliseconds) to "freeze" the atmospheric turbulence and capture the light while it is still forming coherent interference patterns at the detector (Knox and Thompson 1974, Lohmann *et al.* 1983, Roddier 1986). Details of the procedure followed in observing Titan can be found in Gibbard *et al.* (1999, 2004).

With the recent development of adaptive optics on large telescopes, it is possible to improve on the efficiency of speckle imaging with similar spatial resolution. The advantages of AO imaging compared to speckle imaging include the elimination of the need for multiple image frames, and the ability to image fainter objects. An adaptive optics system corrects for turbulence in the Earth's atmosphere by sampling the wavefront and applying a correction based on the distortion measured for a known source within the same isoplanatic patch as the science target (for example, a point source such as a star). Further details on the design and performance of adaptive optics systems can be found in *e.g.* Hardy (1998). The Keck AO system uses a Shack-Hartmann wavefront sensor and a 349-actuator deformable mirror which operates in a closed-feedback loop, at a rate of 500-600 Hz for our Titan observations. For this system Titan itself can serve as a reference source and there is no need for a nearby star.

Titan was observed in broadband K' (1.955-2.292 μm) on fifteen days in 1996-2004, as detailed in Table 1. All individual speckle images have been published in Gibbard *et al.* (1999,2004). In February 2001, March 2003, and February 2004, we observed Titan with the Keck adaptive optics system. In 2001 we used the slit-viewing camera SCAM on the NIRSPEC spectrograph. SCAM is a 256 X 256 HgCdTe PICNIC array (McLean *et al.* 2000) which has a platescale of 0.0167"/pixel. The 2003 and 2004 observations used the NIRC2 camera with a platescale of 0.01"/pixel. The resulting images are shown in Fig.1. The spatial resolution achieved ranged from 0.058 to 0.07" for the speckle images, and 0.045-0.067" for the AO images. The data were processed according to standard infrared data reduction techniques, as described in e.g., Gibbard *et al.* 2004. We obtained an average of 15.8 resolution elements across the disk, ranging from 13.1-18.4 depending on the night of observation. This corresponds to 280-393 km on the surface of Titan at the center of Titan's disk.

Some of our speckle images taken in the period 1996-1998 showed evidence for clouds (Gibbard *et al.* 2004); these images were omitted from the analysis and are not listed in Table 1. None of the AO images presented here showed evidence of clouds.

3 Atmosphere model and surface albedo

In order to separate the light reflected from the surface of Titan from light backscattered from atmospheric haze, we have previously (Gibbard *et al.* 1999) used a radiative transfer model that simulates the absorption/scattering of photons in Titan's atmosphere and the reflection of photons from a constant-albedo surface (Toon *et al.* 1989). Because the depth of Titan's atmosphere (~ 1000 km) is comparable to its radius (~ 2475 km) there are effects at the limb of the satellite that are not properly accounted for in a plane-parallel approximation (Lebonnois and Toublanc 1999). To investigate this effect, Tran and Rannou (2003) have compared the results of the Toon *et al.* code to the results from a 3-D Monte Carlo simulation at wavelengths of 2 μm. They find that there is indeed a discrepancy between the plane-parallel code and the Monte Carlo code near the limb of Titan (although the two codes agree well near the center of the disk), and that a simple geometric correction factor applied to the Toon *et al.* code produces excellent agreement with the Monte Carlo code. We have adopted that correction factor in this work, and have also re-analyzed the data from 1996 (published in Gibbard *et al.* 1999) with the correction.

The model is structured as follows: The total optical depth of the haze layers, τ, is divided among ten layers in the atmosphere at altitudes of 90-180 km, with a maximum at 90 km and decreasing exponentially in the higher layers (Rannou *et al.* 2002). The exact structure of the haze profile is not crucial for this broadband filter; the most important parameter is the total haze optical depth. Free parameters are the values of τ at the south pole, the equator, and the north pole. The haze optical depth is assumed to vary linearly between these points. Methane absorption is parameterized by assuming the gas to be completely absorbing within the fraction of the filter that is in the methane band (59%, Gibbard *et al.* 2004) and to be transparent outside of the methane absorption band.

Model fitting thus involves the variation of three parameters: the total haze optical depth of the south, equator, and north. Once the best-fit haze parameters were determined, the model was used to generate an "atmosphere-only" image with a surface albedo of zero.

This atmosphere-only map was then subtracted from our data to produce an image of the residual emission due to the satellite's heterogeneous surface. The image was calibrated by dividing the residual emission by the residual emission expected from a surface of constant albedo a (we used the value 0.1), then multiplying by the factor a. Further details of the atmosphere model and fitting procedure, as well as sources of error in this approach, can be found in Gibbard *et al.* (1999).

The surface albedoes resulting from the model atmosphere subtraction were projected onto a latitude-longitude grid to produce a surface map, using the central 60 degrees of each image's longitude and latitude. (Fig. 1, bottom). For all longitudes we have overlapping coverage from multiple nights (ranging from 2 to 9 images), which were mean averaged to produce the final surface albedo map.

Titan's leading hemisphere, as noted a decade ago (Lemmon *et al.* 1993, Griffith 1993), is considerably brighter than the trailing hemisphere. This is primarily due to a relatively bright feature centered near 90° longitude. This feature appears to have several centers of brightness, elongated in longitude, with a 'tail' extending somewhat further south around 80°. There is also a bright region in the northern hemisphere around 170 degrees longitude, and another bright feature in the south near 20 degrees longitude (visible in Fig. 1 in the center of the images from March 9 2003 and February 7 2004). The equatorial region of the trailing hemisphere appears very dark; in the longitude range of 180 to 300° we find its reflectance to be quite low, in the range of 0-0.04.

The values we find for Titan's surface albedo are consistent with those found by Gibbard *et al.* (2004) using the DISORT radiative transfer model. This is in contrast to values derived by Coustenis *et al.* 1995 (0.24 for the bright terrain and 0.17 for the dark terrain) and Lemmon *et al.* 1995 (0.27 for the bright terrain and 0.07 for the dark terrain), and more comparable to the values derived by Griffith *et al.* 1991 (0.08-0.09 for the disk-integrated albedo) and Bouchez *et al.* 2000 (surface albedo values ranging from 0.07-0.15). It is clear that Titan's surface is heterogenous and that there is a large albedo contrast between features such as the bright region near 90° longitude and the much darker equatorial region on the trailing hemisphere. The darkest areas on Titan are consistent with low-lying terrain covered by solid or liquid hydrocarbons.

In the simplest interpretation, Titan's surface has two different types of terrain: dark and bright (*e.g.* Lorenz and Lunine 1997). While we do find evidence for these types of terrain (relatively bright terrain with albedo 0.1 on the leading hemisphere and regions with albedo < 0.04 primarily in the equatorial regions on the trailing hemisphere), we also can conclude that there are regions with albedos intermediate between these values, for example at mid-latitudes on the trailing hemisphere. One explanation for the intermediate albedo is that these regions are covered by a mixture of the bright and dark material.

Although observations taken in several spectral windows are consistent with the presence of water ice on Titan's surface (Griffith *et al.* 2003), Coustenis *et al.* (2001) suggest that the bright material on Titan's leading hemisphere is not pure water ice, which should not appear bright at both 1.6 and 2 microns. They suggest the bright area may be water ice combined with methane or ethane frost and organic materials. However, it has been shown by Lorenz and Lunine (2002) that methane frost is not likely to occur below 14 km altitude on Titan.

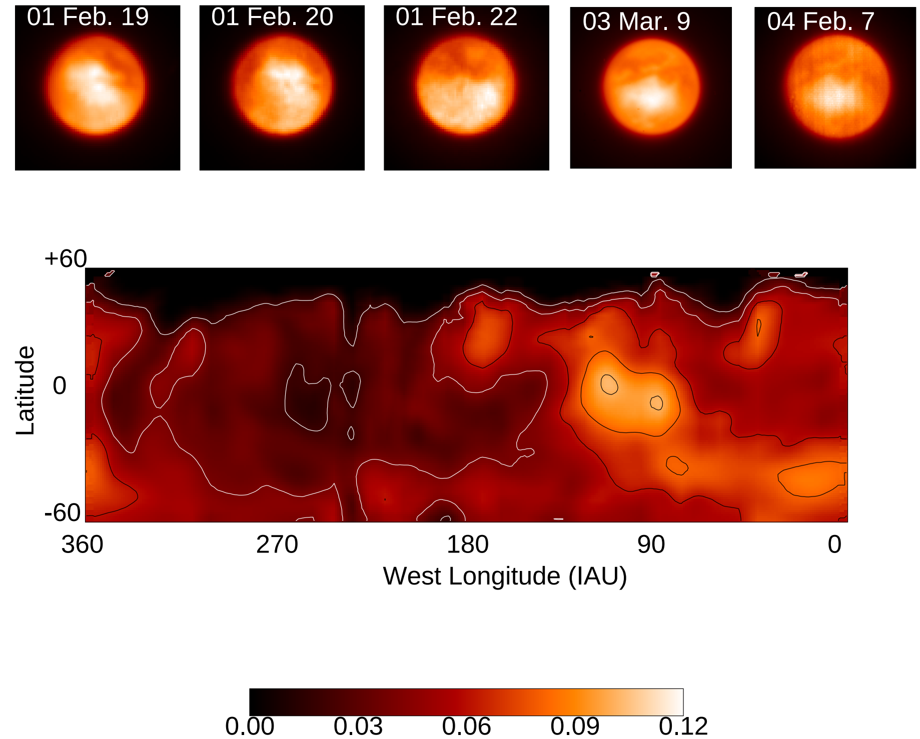

Figure 1: (top) 2 μm images from each of the five nights of adaptive optics observations. The speckle images discussed in this paper can be found in Gibbard *et al.* (2004). Sky north is up, sky east is to the left. Details on each image can be found in Table 1. These images, along with speckle images published in Gibbard *et al.* (2004), were used to construct a surface albedo map (bottom). The map shows Titan's surface reflectivity; contours are 0.02,0.04,0.06,0.08 and 0.10.

4 Titan's haze optical depth in the near-infrared

In the period from 1996-2001 Titan's increased southern limb brightening compared to the northern limb indicated a greater haze optical depth at 2 μm in the southern hemisphere than in the north. This appears to be a seasonal effect, with maximum haze optical depth shifting from pole to pole during Saturn's 30-year orbital period around the Sun (Lorenz *et al.* 1999). In 1980, Voyager observations showed that the northern hemisphere of Titan was darker than the south at visible wavelengths (Sromovsky *et al.* 1981). Since Titan's haze is absorbing at these wavelengths, this implies greater haze optical depth in the north at that time. Observations by the HST over the period from 1994-2000 (Lorenz *et al.* 2001) indicated that seasonal changes in Titan's haze distribution had occurred at visible and near-infrared wavelengths up to 889 nm. They suggest that Titan's seasonal cycle of haze redistribution has an altitude-dependent phase lag, such that the haze at higher altitudes is redistributed before haze at lower altitudes. This would be consistent with a mechanism of pole-to-pole Hadley cell transport of high-altitude haze.

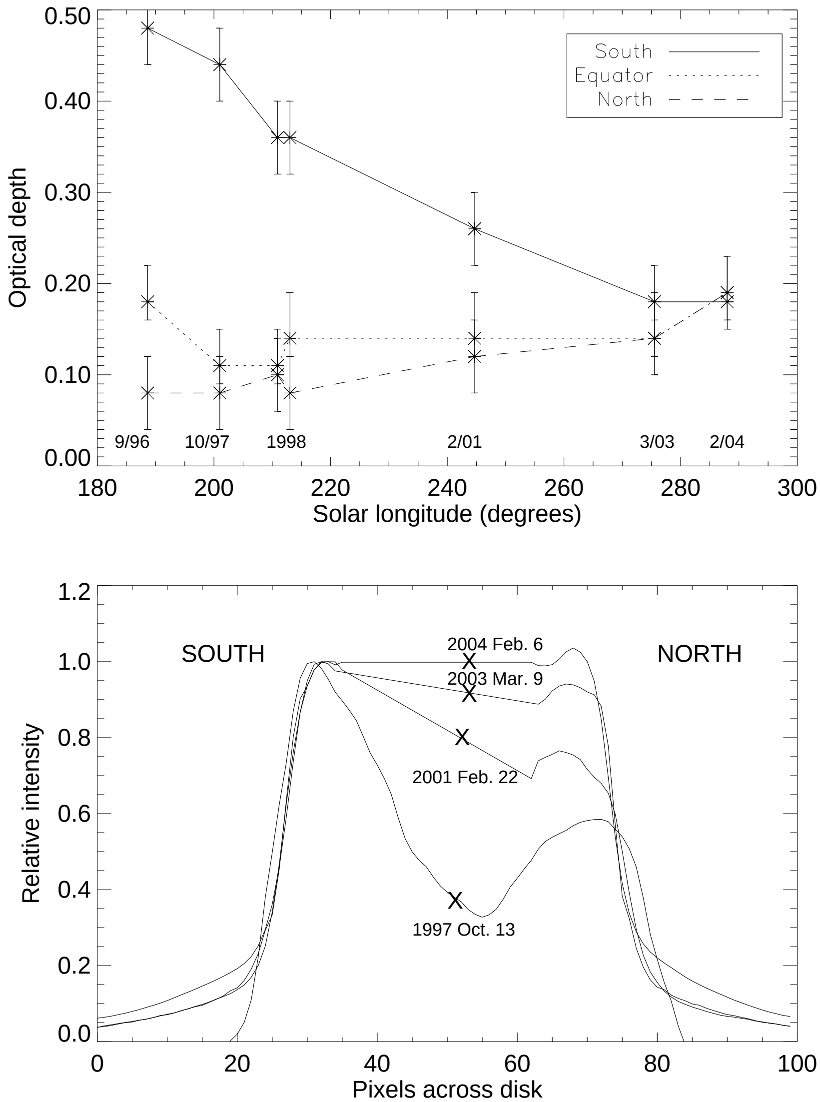

Figure 2: (Top) 2μ haze optical depth values over the span of September 1996-February 2004. Error bars are derived as discussed in Gibbard *et al.* (1999). (Bottom) North/south scans across the center of Titan images from 1997-2004 showing how the haze asymmetry has changed during this time. Surface features have been removed (except for the 1997 data) and replaced with a linear fit. The scans are normalized to the southern limb brightness. Location of the equator is marked by 'X'.

Our own observations support the idea that Titan's broadband 2 μm haze asymmetry has been decreasing over the period from 1996-2004, primarily due to a decrease in the southern haze. As Fig. 2 shows, the southern haze optical depth has decreased from 0.48 to 0.18 over this time, to the point that the southern and northern haze optical depths are currently equal (within error bars). Changes in the equatorial and northern haze optical depths have been been gradual, the equatorial haze remaining essentially constant, while the northern haze has undergone an increase in the last few years of observation. If this trend continues, the northern haze optical depth will soon surpass the southern haze even at low altitudes.

5 Conclusions

Our observations of Titan using the W.M. Keck Observatory adaptive optics and speckle imaging in a 2-micron broadband filter over a period of one-quarter of a Saturnian year have allowed us to obtain full high-spatial-resolution coverage of Titan's surface and to detect predicted changes in Titan's haze distribution. By updating a plane-parallel code to agree with results from Monte Carlo calculations we have improved our modeling of the limbs of the satellite and thus our ability to subtract the contribution of light from the satellite's atmosphere. This allows us to construct a calibrated surface albedo map. We note that the north/south haze optical depth asymmetry in Titan's atmosphere has gradually disappeared in 1996-2004, primarily due to a decrease in the southern haze optical depth. Further improvements in modeling will occur in the future based on data from the Cassini/Huygens mission, which will give us a better idea of the vertical structure in Titan's atmosphere.

ACKNOWLEDGEMENTS

Data presented herein were obtained at the W.M. Keck Observatory, which is operated as a scientific partnership among the California Institute of Technology, the University of California and the National Aeronautics and Space Administration. The Observatory was made possible by the generous financial support of the W.M. Keck Foundation. The authors wish to recognize and acknowledge the very significant cultural role and reverence that the summit of Mauna Kea has always had within the indigenous Hawaiian community. We are most fortunate to have the opportunity to conduct observations from this mountain.

This work has been supported by the National Science Foundation Science and Technology Center for Adaptive Optics, managed by the University of California at Santa Cruz under cooperative agreement No. AST-9876783.

I. de Pater was funded in part by the Miller Institute for Basic Research in Science at the University of California in Berkeley, and by NSF grant NSF AST-0205893.

This research was performed under the auspices of the U.S. Department of Energy, National Nuclear Security Administration by the University of California, Lawrence Livermore National Laboratory under Contract W-7405-ENG-48.

REFERENCES

Bouchez, A.H., M.E. Brown, C.A. Griffith, and R.G. Dekany (2000), Spatially resolved spectroscopy of Titan's surface and atmosphere, American Astronomical Society, DPS Meeting #32, #17.02.

Brown, M.E., A.H. Bouchez, and C.A. Griffith (2002), Direct detection of variable tropospheric clouds near Titan's south pole, *Nature, 420*, 795-797.

Combes, M. L. Vapillon, E. Gendron, A. Coustenis, O. Lai, R. Wittemberg, and R. Sirdey (1997), Spatially resolved images of Titan by means of adaptive optics, *Icarus 129*, 482-497.

Coustenis, A., E. Gendron, O. Lai, J.-P. Veran, J. Woillez, M. Combes, L. Vapillon, T. Fusco, L. Mugnier and P. Rannou (2001), Images of Titan at 1.3 and 1.6 μm with Adaptive Optics at the CFHT, *Icarus, 154*, 501-515.

Coustenis, A., E. Lellouch, J.P. Maillard, and C.P. McKay (1995), Titan's surface: composition and variability from the near infrared albedo, *Icarus 118*, 87-104.

Gibbard, S.G., B. Macintosh, D. Gavel, C.E. Max, I. de Pater, H.G. Roe, A.M. Ghez, E.F. Young and C.P. McKay, (2004), Speckle imaging of Titan at 2 microns: surface albedo, haze optical depth, and tropospheric clouds 1996-1998, *Icarus*, in press.

Gibbard, S.G., B. Macintosh, D. Gavel, C.E. Max, I. de Pater, A.M. Ghez, E.F Young, and C.P. McKay, (1999), Titan: high-resolution speckle images from the Keck Telescope. *Icarus 139*, 189-201.

Griffith, C.A., T. Owen, T.R. Geballe, J. Rayner, and P. Rannou (2003), Evidence for the exposure of water ice on Titan's surface. *Science 300*, 628-630.

Griffith, C.A. (1993), Evidence for surface heterogeneity on Titan, *Nature 364*, 511-514.

Griffith, C.A., T. Owen, and R. Wagener (1991), Titan's surface and troposphere, investigated with ground-based near-infrared observations, *Icarus 93*, 362-378.

Hardy, J.W. (1998), Adaptive Optics for Astronomical Telescopes, Oxford Univ. Press, New York.

Knox, K. T. and B.J. Thompson (1974), Recovery of images from atmospherically degraded short-exposure photographs, *Astrophys. J. 193*, L45-48.

Lebonnois, S., and D. Toublanc (1999), Actinic fluxes in Titan's atmosphere, from one to three dimensions: Application to high-latitude composition, *JGR 104*, 22025-22034.

Lemmon, M.T., E. Karkoschka, and M. Tomasko (1995), Titan's rotational lightcurve, *Icarus 113*, 27-38.

Lemmon, M.T., E. Karkoschka, and M. Tomasko (1993), Titan's rotation: surface feature observed, *Icarus 103*, 329-332.

Lohmann, A., G. Weigelt, and B. Wirnitzer (1983), Speckle masking in astronomy - Triple correlation theory and applications, *Applied Optics 22*, 4028-4037.

Lorenz, R.D., M.T. Lemmon, P.H. Smith and G.W. Lockwood (1999), Seasonal change on Titan observed with the Hubble Space Telescope, *Icarus 142*, 391-401.

Lorenz, R.D., and J.I. Lunine (2002), Titan's snowline, *Icarus 148*, 557-559.

Lorenz, R.D., and J.I. Lunine (1997), Titan's surface reviewed: the nature of the bright and dark terrain, *Planet. Space Sci. 45*, 981-992.

Lorenz, R.D., E.F. Young, and M.T. Lemmon (2001), Titan's smile and collar: HST observations of seasonal change 1994-2000, *GRL 28*, 4453-4456.

McLean, I., J.R. Graham, E.E. Becklin, D.F. Figer, J.E. Larkin, N.A. Levenson, and H.I. Teplitz (2000), Performance and results with the NIRSPEC echelle spectrograph on the Keck II Telescope, *Proc. SPIE 4008*, 1048-1055.

Meier, R., B.A. Smith, T.C. Owen, and R.J. Terrile (2000), The surface of Titan from NICMOS observations with the Hubble Space Telescope, *Icarus 145*, 462-473.

Rannou, P., F. Hourdin, and C.P. McKay (2002), A wind origin for Titan's haze structure, *Nature 418*, 853-856.

Roddier, F. (1986), Triple correlation as a phase closure technique, *Optics Communications 60*, 145-148.

Roe, H.G., I. de Pater, B.A. Macintosh and C.P. McKay (2002), Titan's clouds from Gemini and Keck adaptive optics imaging, *Ap. J. 581*, 1399-1406.

Smith, P.H., M.T. Lemmon, R.D. Lorenz, L.A. Sormovksy, J.J. Caldwell and M.D. Allison, (1996), Titan's surface, revealed by HST imaging, *Icarus 119*, 336-349.

Sromovsky, L.A., V.E. Suomi, J.B. Pollack, R.J. Kraus, S.S. Limaye, T. Owen, H. E. Revercomb, and C. Sagan (1981), Implications of Titan's north-south brightness asymmetry, *Nature 292*, 698-702.

Toon, O.B., C.P. McKay, T.P. Ackerman, and K. Santhanam (1989), Rapid calculation of radiative heating rates and photodissociation rates in inhomogenous multiple scattering atmospheres, *JGR 94*, 16287-16301.

Tran, T. T., and P. Rannou (2003). Comparing 3D spherical Monte-Carlo and 2-stream parallel plane simulation of far-field backscattering image of Titan. *Notes du Pôle de Planétolgie* December 2003, Note #2.